Thermal-induced nonlinear optical characteristics of ethanol solution doped with silver nanoparticles

Zhengle Mao (毛峥乐)[1,2], Lingling Qiao (乔玲玲)[1,2], Fei He (何 飞)[1,2], Yang Liao (廖 洋)[1,2], Chen Wang (王 琛)[1*], and Ya Cheng (程 亚)[1]**

[1] *State Key Laboratory of High Field Laser Physics, Shanghai Institute of Optics and Fine Mechanics, Chinese Academy of Sciences, Shanghai 201800, China*

[2] *Graduate University of Chinese Academy of Sciences, Beijing 100049, China*

[*] *E-mail: wangchen@mail.siom.ac.cn;* [**] *e-mail: ycheng-45277@hotmail.com*

Received January 6, 2009

The investigation of nonlinear optical characteristics of ethanol solution doped with silver nanoparticles is presented. A large thermal-induced third-order nonlinear refractive index up to -1.941×10^{-7} cm^2/W is obtained from the mixed solution under 488-nm continue wave (CW) laser irradiation, which may result from surface plasmon resonance (SPR) enhancement effect of silver nanoparticles as well as high thermo-optic coefficient and low thermal conductivity of ethanol. Obvious spatial self-phase modulation and influence of thermal-induced negative lens effect are observed when a beam propagates through this solution, indicating promising applications such as optical limiting, beam flattening, and so on.

OCIS codes: 190.0190, 160.4330, 160.4236, 240.6680.

doi: 10.3788/COL20090710.0949.

Materials with high third-order nonlinear refractive index are always of large interests for their potential applications on many nonlinear optical devices such as optical limiting, beam flattening, optical switching, weak absorption measurement, spatial dark soliton transmission[1−4], and so on. Composite systems containing metal nanoparticles such as Ag, Au, and Cu are the promising solutions to this end because of metal nanoparticles' unique ability to support surface plasmon resonance (SPR) at visible wavelengths, which in turn can give rise to a giant enhancement of nonlinear optical response in media[5−8]. Especially, Ag nanoparticles attract the most concerns because they can provide the largest enhancement factor of SPR among all kinds of metal nanoparticles[9]. In the past several years, it has been widely reported that Ag nanoparticles were embedded into solid matrices such as silica glass[10] and sapphire[5] or doped into liquids[11−15] to enlarge the third-order optical nonlinear response successfully. Those works show a prospect of controlling the optical response of media with the aid of Ag nanoparticles. In this letter, we study the nonlinear optical characteristics of ethanol solution doped with Ag nanoparticles. A very large thermal-induced third-order nonlinear refractive index of this mixed solution is measured to be -1.941×10^{-7} cm^2/W under 488-nm continuous-wave (CW) laser irradiation, which is about one order of magnitude higher than the result reported so far[16]. The large thermal-induced nonlinearity and the effect of a thermal-induced negative lens are further demonstrated by diffraction patterns.

In our experiment, Ag colloid was prepared by the chemical reaction methods reported by Lee *et al.*[17]. 9-mg silver nitrate was added into 50-ml distilled water. The solution was heated to its boiling point and 1-ml 1% sodium citrate was added. Then, the solution was boiled for 20 min. Ag colloid was obtained after cooling down the solution at room temperature and its concentration was about 1.08×10^{-3} mol/L. Figure 1 shows the absorption spectra of Ag colloid. It can be seen that the absorption peak of SPR is around 455 nm. The average size of nanoparticles was about 50 nm by electron microscopy imaging. Ag colloid was doped into ethanol and distilled water with volume rates of 1:4 and 1:1, respectively. These two kinds of mixed solutions were indicated by Ag:ethanol and Ag:water in the following.

Conventional closed-aperture and open-aperture z-scan techniques[18] were adopted to investigate the nonlinear refractive index and nonlinear absorption respectively. Figure 2 is the schematic diagram of z-scan experiment setup. To optimize the SPR effect of Ag nanoparticles, a tunable CW Arion laser (Griot Mell, USA) at a wavelength of 488 nm was chosen to irradiate the sample.

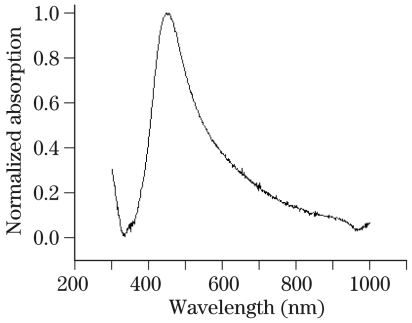

Fig. 1. Absorption spectrum of Ag colloid.

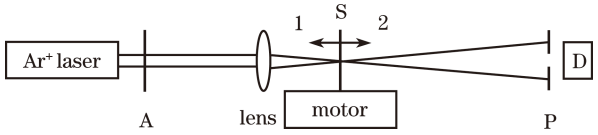

Fig. 2. Schematic diagram of z-scan experimental setup. A, attenuator; S, ethanol solution of silver nanoparticles; P, aperture; D, detector.

The transmittance difference between normalized peak and valley $\Delta T_{\rm p-v}$ (defined by $T_{\rm p}-T_{\rm v}$), on-axis phase shift $\Delta\Phi$, and thermal-induced third-order nonlinear refractive index n_2 are associated by equations as follows[18]:

$$\Delta T_{\rm p-v} = 0.406(1-S)^{0.25}\Delta\Phi, \quad (\Delta\Phi < 2\pi) \tag{1}$$

$$\Delta\Phi = kL_{\rm eff}n_2I_0 = (2\pi/\lambda)L_{\rm eff}n_2I_0, \tag{2}$$

$$S = 1-\exp\left(-2\frac{r}{w_{\rm a}}\right), \tag{3}$$

$$L_{\rm eff} = [1-\exp(-\alpha L)]/\alpha, \tag{4}$$

where λ is the wavelength of laser, I_0 is the intensity of beam at focus, r is the aperture radius, $\omega_{\rm a}$ is the beam radius on aperture position, α is the linear absorption coefficient, and L is the sample thickness. In closed-aperture z-scan measurement, the laser beam was focused by a lens of 180-mm focal length, and the solutions under investigation were contained in a 1-mm-thick quartz cell which was mounted on a step motor (Zolix, China) and translated along the beam direction. The emergent light from the solutions was detected by a power meter (Coherent, USA). For open-aperture measurement, the aperture was just replaced by a lens of 100-mm focal length to collect almost all transmitted light into detector to study the nonlinear absorption. Another 30-mm-thick quartz cell was used in the study of spatial self-phase modulation and nonlinear absorption properties of the solutions.

Figure 3 shows the result of closed-aperture measurement. The feature of "peak followed by valley" indicates the self-defocusing, in other words, negative nonlinear refractive index. The absorption coefficient of Ag:ethanol was measured to be 0.84 $\rm cm^{-1}$ while the absorption coefficient of pure ethanol was nearly negligible, which demonstrated that strong absorption of mixed solution mainly came from SPR of silver nanoparticles. A low input power of 2 mW was used since it was enough to create measurable signal. According to Eqs.(1)–(4), the third-order nonlinear refractive index of Ag:ethanol was calculated to be -1.941×10^{-7} $\rm cm^2/W$. To interpret this large nonlinear refractive index, we propose the following physics picture. Due to SPR of silver nanoparticles doped in solutions, light energy is absorbed significantly by silver nanoparticles and then transferred to liquid through the non-irradiative relaxation to ground state, which leads to the increase of local temperature in the solution. Then the temperature gradient filed results in a change of the local refractive index because the local refractive index decreases with the increase of temperature for most liquids such as ethanol and water. Especially with 488-nm CW laser irradiation which is near the resonance absorption peak of Ag nanoparticles, SPR is intense and heat is effectively accumulated. Therefore, the large thermal-induced negative third-order nonlinear refractive index is produced.

For comparison, we performed the closed-aperture z-scan experiment of pure ethanol without silver nanoparticles under the same experimental conditions, and the feature of "peak followed by valley" dissappeared, which clearly indicated that silver nanoparticles enhanced the thermal-induced nonlinearity. We also conducted the

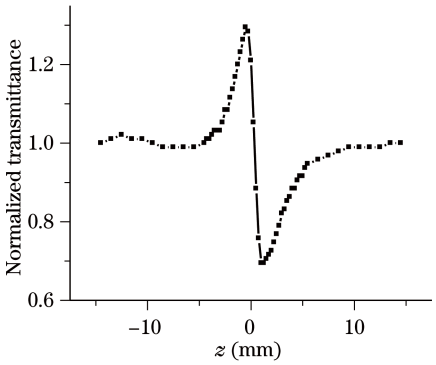

Fig. 3. Curve of closed-aperture z-scan measurement.

Table 1. Thermal-Optical Properties of Ethonal and Water

Material	κ (W/(m · K))	$\rm d$$n$/d$T$ ($\rm K^{-1}$)
Ethanol	0.168	-4×10^{-4}
Water	0.56	-1×10^{-4}

measurement of Ag:water. In order to obtain measurable signal, the input power was increased to about 20 mW. The third-order nonlinear refractive index of Ag:water was obtained to be -3.81×10^{-8} $\rm cm^2/W$, which was in good agreement with the value reported in Ref. [16]. The thermal-induced third-order nonlinear refractive index n_2 also could be quantitatively estimated by the thermal nonlinear optical theory[19] as

$$n_2 = \frac{{\rm d}n}{{\rm d}T}\frac{\alpha\omega_o^2}{\kappa}, \tag{5}$$

where $\frac{{\rm d}n}{{\rm d}T}$ is the thermo-optic coefficient, κ is the thermal conductivity, and ω_o is the waist width at focus. Based on the absorption coefficients measured in experiment and the parameters in Table 1[19,20], the theoretical values of n_2 in Eq. (5) are calculated as -1.80×10^{-7} and -5.58×10^{-8} $\rm cm^2/W$ for Ag:ethanol and Ag:water, respectively, which are in good agreement with the measured values. The fact that ethanol exhibits higher thermo-optic coefficient and lower thermal conductivity than water should be responsible for the result that the thermal-induced third-order refractive index of Ag:ethanol is one order of magnitude larger than those of Ag:water both in our experiment and the one reported in Ref. [16].

The curve of open-aperture measurement in Fig. 4 shows both saturated absorption and inverse saturated absorption in Ag:ethanol. In order to further clarify the nonlinear absorption behavior, we used a 30-mm-thick quartz cell containing Ag:ethanol and studied the dependence of transmittance on the incident power. Similar to the result in Fig. 4, Fig. 5 also shows both saturated absorption and inverse saturated absorption. When the input power was lower than about 7.5 mW, the transmittance decreased with the increase of input power and *vice versa*. The inverse saturated absorption occurred at low input power, which was similar to the situation reported in Ref. [15]. Whereas the saturated absorption occurring at higher input power may be ascribed to two factors: SPR was so intense under 488-nm wavelength that it reached saturation at relatively low input power; and due

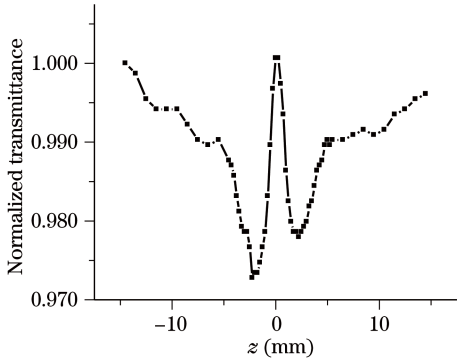

Fig. 4. Curve of open-aperture z-scan measurement.

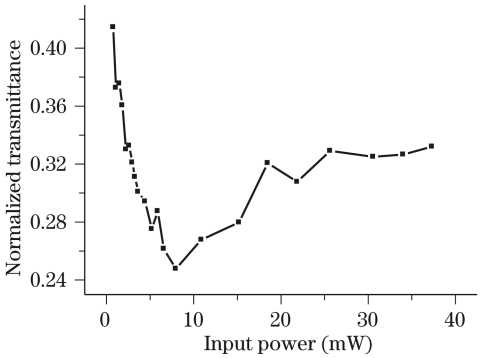

Fig. 5. Transmittance dependence on input power of ethanol solution doped with silver nanoparticles.

to the low thermal conductivity of ethanol and CW laser irradiation, the effective heat accumulation inhibited the further absorption of silver nanoparticles. For comparison, Ag:water was measured in open-aperture z-scan experiment under the input power of 20 mW, and no saturated absorption was observed since the thermal conductivity of water was 3.3 folds higher than that of ethanol.

Furthermore, to verify the large thermal-induced third-order nonlinear refractive index of Ag:ethanol, we studied the spatial self-phase modulation when a laser beam propagated through this mixed solution. Figure 6 shows a set of spatial diffraction patterns of emergent laser when the incident plane of Ag:ethanol solution was placed in front of (but close) to the focus (position 1 in Fig. 2). A high input power of tens of milliwatts was applied to produce large thermal effect and different concentrations were adopted in order to find out the optimum concentration for the largest thermal-induced phase shift. When the beam propagated through the solution, thermal-induced nonlinear phase shift was accumulated gradually according to Eq. (2) and produced the so-called spatial self-phase modulation. Spatial self-phase modulation occurs when a beam of non-uniform intense distribution such as a Gaussian beam propagates in a nonlinear medium and a nonlinear refractive index is created. The change of refractive index conversely changes the transverse phase of the beam. When the phase shift is accumulated to a certain degree, the transverse distribution of emergent laser will vary significantly. Especially under the high input power, spatial self-phase modulation could be studied throughout the visible diffraction pattern of emergent laser. The number of rings is determined by the amount of phase shift induced by thermal-induced nonlinearity according to[21]

$$\Delta\Phi = N \cdot 2\pi, \tag{6}$$

where N is the number of diffraction light rings. So many rings in Figs. 6(b)–(f) indicate that a large phase shift is created according to Eq. (6). With the change of concentration, the number of rings changes and reaches its maximum when the volume ratio of Ag colloid and ethanol is about 1:4. We conjecture that, when the concentration is relatively low, the more the silver nanoparticles exist, the stronger the absorption caused by SPR is. However, when the concentration is further increased to a certain degree, the absorption and scattering that occurr in the forepart of optical path would greatly reduce the light intensity, and consequently, the SPR in the residual part of optical path. Furthermore, the total phase shift is decreased since phase shift is a process of accumulation through the whole optical path. Hence, it is reasonable to expect that the optimal concentration for the largest phase shift should be different for the solutions of different thicknesses. For comparison, lenses with different focal lengthes of 30, 100, and 180 mm were used to focus the incident laser in our experiment, and the lens with 180-mm focus length lens was found to create the largest number of diffraction rings, which demonstrated that lens of a longer focal length may be beneficial to the phase shift accumulation.

When we changed the position of solution, there appeared an interesting and obvious variation of diffraction patterns. Figures 6(b)–(f) show a tightly focused light spot surrounded by diffraction rings, whereas Fig. 7(a) shows a large dark circular central area surrounded by the diffraction rings when the front face of the cell is moved behind (but close to) the focus (position 2 in Fig. 2), whose transverse intensity distribution is shown in Fig. 7(b). Since the solution plays a role of a negative lens, the situations in Figs. 6 and 7 correspond to the ones where a convergent and a divergent Gaussian beams passed through a negative lens, respectively. A theoretical calculation of the diffraction patterns for these two situations has been reported in Ref. [22], which agreed well with that observed in our experiment. It is clearly demonstrated in Fig. 7(b) that the effect of thermal-induced negative lens can be applied on optical limiting and optical flattening.

In conclusion, we report a systematic investigation on the thermal-induced optical nonlinearity of ethanol

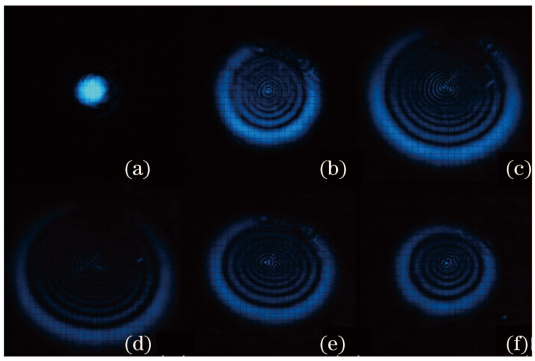

Fig. 6. Number of rings changes when Ag colloid is added gradually. (a) 2-ml pure ethanol; (b)–(f) 0.2, 0.4, 0.6, 0.8, and 1 ml of Ag colloid are added into 2-ml ethanol, respectively.

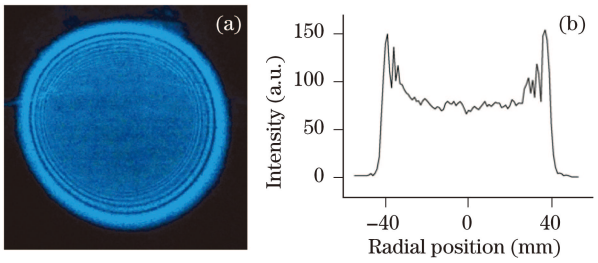

Fig. 7. When the sample is placed in front of and close to focus, effects of optical limiting and optical flattening are obvious. (a) Original pattern; (b) transverse intensity distribution.

solution doped with silver nanoparticles. A large thermal-induced third-order nonlinear refractive index is measured to be -1.941×10^{-7} cm^2/W with z-scan technique. The large thermal nonlinearity is attributed to not only the intense SPR of silver nanoparticles but also the high thermo-optic coefficient and low thermal conductivity of ethanol. Spatial self-phase modulation and thermal-induced negative lens effect are clearly observed. The dependence of thermal-induced phase shift on concentration is also systematically studied. This self-action effect of thermal-induced negative lens will be useful for many applications such as optical limiting, beam flattening, and so on.

This work was supported by the National Basic Research Program of China (No. 2006CB06000b) and the National Natural Science Foundation of China (No. 10804116). Y. Cheng acknowledges the supports of 100 Talents Program of the Chinese Academy of Sciences, Shanghai Pujiang Program, and National Outstanding Youth Foundation.

References

1. O. Durand, V. Grolier-Mazza, and R. Frey, Opt. Lett. **23,** 1471 (1998).
2. J. Staromlynska, T. J. McKay, and P. Wilson, J. Appl. Phys. **88,** 1726 (2000).
3. G. B. Al'tshuler and M. V. Inochkin, Phys. Usp. **36,** 604 (1993).
4. X. Chen, Y. Chen, Q. Li, J. Zhang, and J. Huang, Acta Opt. Sin. (in Chinese) **16,** 952 (1996).
5. R. A. Ganeev, A. I. Ryasnyanskiĭ, A. L. Stepanov, T. Usmanov, C. Marques, R. C. da Silva, and E. Alves, Opt. Spectrosc. **101,** 615 (2006).
6. S. Debrus, J. Lafait, M. May, N. Pinçon, D. Prot, C. Sella, and J. Venturini, J. Appl. Phys. **88,** 4469 (2000).
7. X. Qu, J. Liang, C. Yao, Z. Li, J. Mei, and Z. Zhang, Chinese J. Lasers (in Chinese) **34,** 1459 (2007).
8. X. Qu, J. Wang, C. Yao, and Z. Zhang, Chin. Opt. Lett. **6,** 879 (2008).
9. J. Yang, J. Zhou, K. Wang, and Q. Zhang, Acta Opt. Sin. (in Chinese) **27,** 119 (2007).
10. C. Zheng,Y. Du, M. Feng, and H. Zhan, Appl. Phys. Lett. **93,** 143108 (2008).
11. C. Wang, Y. Fu, Z. Zhou, Y. Cheng, and Z. Xu, Appl. Phys. Lett. **90,** 181119 (2007).
12. E. L. Falcão-Filho, C. B. de Araújo, and J. J. Rodrigues, Jr., J. Opt. Soc. Am. B **24,** 2948 (2007).
13. D. Rativa, R. E. de Araujo, and A. S. L. Gomes, Opt. Express **16,** 19244 (2008).
14. R. A. Ganeev and A. I. Ryasnyansky, Appl. Phys. B **84,** 295 (2006).
15. R. A. Ganeev, M. Baba, A. I. Ryasnyanskiĭ, M. Suzuki, and H. Kuroda, Opt. Spectrosc. **99,** 694 (2005).
16. T. Jia, T. He, P. Li, Y. Mo, and Y. Cui, Opt. Laser Technol. **40,** 936 (2008).
17. P. C. Lee and D. Meisel, J. Phys. Chem. **86,** 3391 (1982).
18. M. Sheik-Bahae, A. A. Said, T.-H. Wei, D. J. Hagan, E. W. van Stryland, IEEE J. Quantum Electron. **26,** 760 (1990).
19. R. W. Boyd, *Nonlinear Optics* (2nd edn.) (Academic Press, London, 2003) p.220.
20. R. C. Kamikawachi, I. Abe, A. S. Paterno, H. J. Kalinowski, M. Muller, J. L. Pinto, and J. L. Fabris, Opt. Commun. **281,** 621 (2008).
21. S. D. Durbin, S. M. Arakelian, and Y. R. Shen, Opt. Lett. **6,** 441 (1981).
22. K. He and L. Deng, High Power Laser and Particle Beams (in Chinese) **15,** 940 (2003).